



# Highly Accurate Directional Overcurrent Coordination via Combination of Rosen's Gradient Projection–Complex Method With GA-PSO Algorithm

Ahmad Darabi , Mehdi Bagheri , *Member, IEEE*, and Gevork B. Gharehpetian , *Senior Member, IEEE*

**Abstract**—This research work involves a highly accurate directional overcurrent coordination using the complex method–Rosen's gradient projection nonlinear programming approach with the genetic algorithm-particle swarm optimization (GA-PSO) metaheuristic optimization algorithm. To accelerate the optimization process, manual tuning steps are proposed to remove miscoordinations quickly and to determine the relay type in the case that different relay curves are given for coordination. In this manner, the metaheuristic and the deterministic parts share their advantages so that their combination leads to a significant tradeoff between exploration and exploitation. In addition, different objective functions for each part are introduced. For various conditions, the proposed method is applied to the eight-bus transmission and 33-kV distribution part of the 30-bus IEEE power system. Next, the superiority of the proposed algorithm over other researches is verified by the observation that the results are in the range of dual setting schemes.

**Index Terms**—Directional overcurrent relay (DOCR), metaheuristic optimization, nonlinear programming (NLP), overcurrent protection.

## I. INTRODUCTION

**D**ESPITE the advantages of distributed generation (DG), such as decrease in the construction of transmission lines, enhancement of the voltage profile, decrease in power losses, contribution to the generation in peak demand, sustainable utilization, and inexpensive energy generation [1]–[3], the presence of DG has led to negative consequences for the power system, particularly for power protection, such as changes of the short circuit level and the direction of fault currents. Among all

the overcurrent protective devices, the overcurrent relay has attracted the most attention in the literature because of economic reasons [4]–[6] and because of its simpler implementation in modern meshed networks relative to reclosers and fuses [7]–[10]. The changes of the fault current direction can be addressed by making overcurrent relays directional, however, challenges associated with variations of the fault current profile cannot be overcome easily. Selectivity, reliability, and fast tripping are important factors in directional overcurrent relay (DOCR) protection. Selectivity means that each relay should react to faults in its corresponding protection zone [11], [12]. This property may be lost when the fault current magnitude changes [3], [13], [14]. Promising advances have been reported on this topic, such as adaptive protection [3], [13]–[16], fault current limiters [1], [17], [18], fast detection of fault current [19], limitations of DG generation capacity [10], fault ride through the control of grid-tied inverters [2], [20], [21], optimal DG placement and sizing [1], [22], planning schemes [17], [23], clustering schemes [24], minimum break point set determination [25], stationary Internet of Things devices [26] or communication assisted dual setting schemes [27], and multiple relay settings based on different DG penetration levels. Each of these proposals has some drawbacks [3]; the common factor among them is that overcurrent coordination must be achieved for at least one fixed configuration of the power network. Addressing this purpose is the focus of this paper. As outlined before, reliability (i.e., each relay should be backed up by other relays) and fast operation are important factors in overcurrent coordination. Faster operation of relays leads to faster isolation of the faulty section, which subsequently blocks the propagation of the fault to the rest of the power network in less time. Moreover, fast operation of DOCRs may lead to reduced damage, enhanced power quality, and prevention of transient instability of the induction or synchronous generators [28], [29]. Consequently, minimization of the total relay operating times is an important objective; as the total relay operating times for a coordination scheme decreases, the algorithm performs better. Furthermore, because of the reliability property of DOCR coordination, each relay has backup protection, and because of the selectivity property, backup relays are designed to operate after their primary relays with a time difference known as the coordination time interval (CTI).

Manuscript received November 8, 2018; revised January 17, 2019; accepted March 6, 2019. This work was supported in part by the Faculty Development Competitive Research Grant of Nazarbayev University under Project SOE2018018 and in part by the Social Policy Grant of Nazarbayev University. (Corresponding author: Ahmad Darabi.)

A. Darabi is with the Department of Electrical Engineering, Technical University of Kermanshah, Kermanshah 6715685420, Iran (e-mail: ad.ahmad@aut.ac.ir).

M. Bagheri is with the Department of Electrical and Computer Engineering, Nazarbayev University, Astana 010000, Kazakhstan (e-mail: mehdi.bagheri@nu.edu.kz).

G. B. Gharehpetian is with the Department of Electrical Engineering, Amirkabir University, Tehran 1591634311, Iran (e-mail: grptian@aut.ac.ir).

Digital Object Identifier 10.1109/JSYST.2019.2904383

This parameter is typically between 0.2 s and 0.5 s and is set to 0.3 s, in this paper. When this setting is violated, the selectivity or fast tripping property is also violated. If the operating time difference between the primary and backup relays is less than the CTI, then nuisance tripping of the backup relay may occur, and unnecessary outage and selectivity violation is expected. Moreover, if this time difference is much greater than the CTI, then the first factor, i.e., minimizing relay operating times, is violated. Thus, the second objective is to minimize this time difference and prevent violation cases. Thus, accurate overcurrent coordination is vitally important for a power system and has attracted strong attention in the literature [3], [6], [17], [30]–[38]. Using the proposed algorithm, significant improvements toward these objectives are achieved, as discussed in detail in the subsequent sections. Generally speaking, overcurrent coordination involves a challenging nonlinear programming (NLP) problem to obtain optimized values for time setting multipliers (TSMs) and plug setting multipliers (PSMs) while satisfying the aforementioned objectives and constraints. Diverse metaheuristic [3], [30]–[35] and deterministic [4], [17], [36], [37], approaches and their combinations [6], [18], [38] have been applied to overcurrent coordination problem in the literature. All metaheuristic approaches have some common properties, and this premise is valid for deterministic approaches, such as linear programming (LP) or NLP. Metaheuristic algorithms can be applied to nonconvex design spaces. These algorithms also search over the global design space, including several convex spaces with different local optima. Moreover, the population-based methods are problem independent. These methods can be applied to linear and nonlinear problems; however, they have some considerable drawbacks. These algorithms have stochastic behavior, and they search over design space randomly. In other words, even for two consecutive computer runs with the same initial points, the final results differ from each other, and the solution may be only a local optimum. To find the best solution, the neighborhood of this solution should be explored. After reaching the vicinity of the global optimum, the algorithm should obtain exact quantities for solutions in a reasonable time. Thus, exploitation becomes more important. The exploitation and exploration tasks are in contrast and complementary to each other; consequently, achieving a balance between them is another challenge associated with population-based algorithms. On the one hand, if a particular metaheuristic method increases exploration and exploitation simultaneously, it could be very time consuming. On the other hand, avoiding constraints from the violation, decreasing primary operation times and reducing discrimination times between primary and back up relays are other responsibilities of metaheuristic techniques. Consequently, the objective functions (OFs) should achieve a balance among these three terms. Relative to deterministic techniques, this aspect is another prominent drawback of population-based methods.

Alternatively, deterministic methods can be used for convex problems in a local optimum vicinity [39]. Relative to stochastic algorithms, these methods are more efficient, more accurate and faster for finding exact local optima, i.e., providing better exploitation. In addition, considering some predefined constraints, these methods can solve linear or nonlinear problems. As a

result, during the iterative process of solving a problem, all constraints remain satisfied, and there is no need to add a penalty term for a fitness function to protect solutions from constraint violations. This characteristic can be considered their prominent advantage since fitness functions can avoid excessive terms. In the case of the LP problem [17], [36], the fitness function can concentrate on minimizing the operation times of primary relays only because in the case of the LP, all OFs and constraints are linear; in the case of NLP [4], [37], the fitness function can focus on both primary operation times and discrimination times simultaneously. Thus, NLP outperforms LP for DOCR coordination schemes. Because of the many differences among NLP methods, in this paper, two of the most appropriate alternatives have been selected. Based on the above introduction, the combination of metaheuristic and deterministic methods can be efficient because metaheuristic methods avoid solutions becoming trapped in local optima and because deterministic methods can both find the best solutions in each convex zone and reduce the fitness function parameters. In particular, the exploration can be accomplished using a metaheuristic method, and exploitation can be accomplished by using a deterministic method. In the current research work, to eliminate the aforementioned deficiencies, metaheuristic, deterministic, and analytic manipulations have been used to solve the overcurrent coordination problem. Clearly, the first step in overcurrent coordination is to remove all violations; this step is achieved by the analytic part quickly (e.g., in a few seconds). After removing all violations by the analytic part, primary operation times and discrimination times without any violation can be optimized by NLP and the metaheuristic parts. After eliminating the violations, the proposed algorithm avoids any future violation because, in the NLP part, violations are considered constraints for NLP; in the metaheuristic part, violations have a large constant (i.e., higher importance) in the OF. Among all deterministic approaches, NLP techniques are more appropriate than LP methods because, in LP algorithms, both OFs and constraints must be linear; consequently, discrimination times cannot be optimized. Rosen's gradient projection (RGP) and the complex method are used as the NLP part of the proposed algorithm because these methods have some advantages over other NLP algorithms, as discussed in detail in subsequent sections of this paper. In the next section, all formulations of the constraints and the OFs are presented. The proposed algorithm is described in detail in Section III. Section IV presents the simulation and results; the results are compared with other research results, and notable observations are discussed. The Section V presents the conclusion.

## II. PROBLEM FORMULATION

### A. Relay Curves

In this paper, overcurrent relay curves given by IEC standard 255-4 [40] are used as

$$t_{op} = \frac{A \times \text{TSM}}{\left(\frac{I_f}{I_{\text{pickup}}}\right)^B} + C \quad (1)$$

where  $I_f$  is the detected fault current by DOCRs and  $I_{\text{pickup}}$  is the pickup load current. DOCRs are classified in three groups of

TABLE I  
IEC STANDARD RELAYS [40]

Relay Type	A	B	C
SI	0.14	0.02	0
VI	13.5	1	0
EI	80	2	0

relays: standard inverse (SI), very inverse (VI), and extremely inverse (EI). Table I presents the A, B, and C coefficients for various types of relays.

### B. Objective Functions

Considering the coordination constraints, suitable OFs can improve the overcurrent protection efficiently. The proposed OFs are given by

$$\text{OF} = \sum_{i=1}^{PN} (k |\Delta t_i - |\Delta t_i|| t_{mi}^2 + (\Delta t_i + |\Delta t_i|) t_{bi}^2) \quad (2)$$

$$\text{O.F}_1 = \sum_{i=1}^{RN} (t_{mi})^2 + \sum_{i=1}^{RN} (\Delta t_i)^2 \quad (3)$$

$$\Delta t_i = t_{bi} - t_{mi} - \text{CTI} \quad (4)$$

where the discrimination time is defined via (4) and the OF is applied to the genetic algorithm-particle swarm optimization (GA-PSO) part;  $\text{O.F}_1$  is applied to the NLP. The major goals of the OF are to prevent creating violations and prepare the solutions submitted to the NLP. In other words, providing different points from the search spaces of TSMs and PSMs and preventing miscoordination are the main duties of the GA-PSO part, and  $t_m^2$  is not optimized independently as with conventional OFs. In contrast, minimizing primary operating times and reducing TSMs and discrimination times are responsibilities of the NLP part by introducing  $\text{O.F}_1$ . In all the equations, when a fault occurs in front of relay  $m$ ,  $t_{mi}$  and  $t_{bi}$  are the primary and secondary operation times for the  $i$ th relay pair, respectively.  $k$  is a positive large constant value (e.g.,  $10^{10}$ ), and  $PN$  and  $RN$  are the total pair numbers and the relay numbers, respectively. All coordination constraints can be summarized by the following equations:

$$\Delta t_i \geq 0 \quad \text{for } i=1:PN \quad (5)$$

$$I_{\text{pickup}} = \text{PSM}_i I_{\text{maxload}i} \quad \text{for } i=1:RN \quad (6)$$

$$1.2 \leq \text{PSM}_i \leq 1.6 \quad \text{for } i=1:RN \quad (7)$$

$$\text{TSM}_{\min} \leq \text{TSM}_i \leq \text{TSM}_{\max} \quad \text{for } i=1:RN. \quad (8)$$

The values for  $\text{TSM}_{\min}$  and  $\text{TSM}_{\max}$  are discussed in Section IV.

## III. PROPOSED ALGORITHM

The proposed algorithm has three metaheuristic, analytic, and deterministic parts.

### A. Metaheuristic Part

The stochastic property is important for the proposed algorithm. The most important dedicated goals of this part can be classified into three groups:

- 1) preventing miscoordination cases,
- 2) introducing diverse TSMs and PSMs in the search space and consequently reducing the possibility of getting trapped in local optima, and
- 3) delivering optimized PSM values to the NLP.

To achieve the first goal, coefficient  $k$  in the OF of (2) is defined as a large positive value to avoid the violated cases. The second goal of the stochastic part is to guarantee the exploration of methods to reach the global optima. Thus, selection of a population-based algorithm with an acceptable exploration is required to find a variety of TSMs and PSMs. However, finding various points is more important and critical for PSM values than TSM quantities because RGP optimizes only TSMs. Consequently, the responsibility of minimizing PSMs should be assigned to the metaheuristic part; this task is the last goal of this part. Generally speaking, the proposed metaheuristic method should provide favorable exploration for both TSM and PSM optimization and desirable exploitation for PSM optimization, since NLP can find the best existing optima for TSMs in a local neighborhood. In the proposed algorithm, GA and PSO are implemented in parallel with each other once per iteration. In other words, when a population is submitted to the metaheuristic part, GA and PSO are applied for the population separately, and then their outputs are sorted based on the OF. Subsequently, the first  $n$  populations with the lowest cost functions are selected, and other populations are removed. Thus, the first population is the global best; moreover, if there are any changes in the so-far global best of each individual particle in the PSO algorithm, then the so-far global bests of the individual particles are updated.

### B. Analytic Part

This part has two important tasks. The first task is to remove all violations and provide a feasible solution to deliver to the metaheuristic and NLP parts quickly. The second task is to determine the relay curve types in the case where different relay types are allowed for overcurrent coordination. This part plays a significant role in reducing the proposed algorithm run time. Although the GA-PSO algorithm can remove violated cases without this part, the process takes considerable time. Thus, by applying this component, the metaheuristic part can be less involved in this task. Moreover, after eliminating all miscoordination by the application of this part, because of NLP and GA-PSO properties, no violation occurs during the algorithm run time; clearly, this part is implemented only once in each overcurrent coordination optimization. In other words, NLP creates feasible solutions in each iteration, and OF does not allow the GA-PSO algorithm to violate the coordination constraints. This strategy saves time, reduces calculation, and makes the algorithm suitable for some applications in which accurate coordination considering a reasonable run time is desired. This part consists of two scenarios, given as follows.

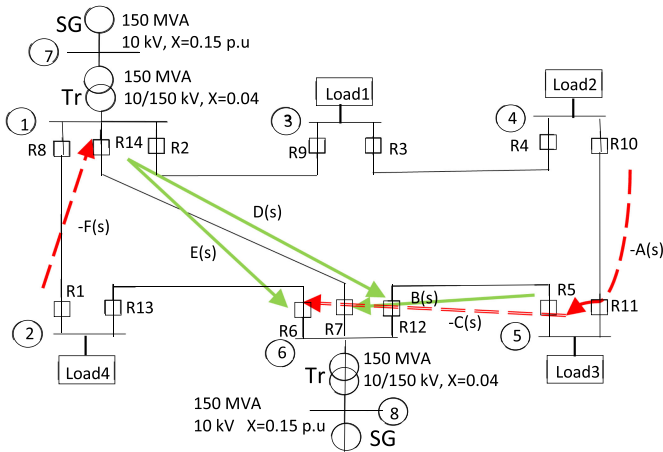


Fig. 1. IEEE 8-bus transmission network.

1) *Scenario 1- Decrease in the Main Relay TSM*: The principle of scenario 1 is to decrease the TSMs of the main relays in violated constraints to eliminate violations. However, although a decrease in the TSMs of the main relays in miscoordinated cases can lead to the removal of those miscoordinations, it can also result in possible miscoordinations in some other pairs, for which these specific relays are their backup protection. The IEEE 8-bus 150-kV transmission network shown in Fig. 1 is given as an illustrative example.

In this figure, black solid lines are electrical lines, red dashed arrows denote relay pairs that are not coordinated, and green solid arrows indicate coordinated relay pairs. All required discrimination times in seconds are shown in the figure as A, B, C, D, E, and F, which are positive constants. In the figure, pairs  $R_1-R_{14}$ ,  $R_{10}-R_{15}$ , and  $R_5-R_6$  not coordinated, and pairs  $R_{14}-R_{12}$ ,  $R_{14}-R_6$ , and  $R_5-R_7$  are coordinated. Assuming that  $E > D$ , then  $R_{14}$  is coordinated with  $R_{12}$  considering the CTI time difference. Consequently,  $D$  becomes zero,  $E$  becomes smaller, and the possibility of removal of miscoordination between  $R_1-R_{18}$  increases. Even if this miscoordination is not cleared, the discrimination time between these relays from a negative value approaches zero. Note that scenario 1 has no effect on pair  $R_{10}-R_5$ . After each change in TSMs, discrimination times are updated in the loop. This scenario checks all violations iteratively until no TSM can be changed. At this point, scenario 2 is implemented. Although scenario 1 appears simple, it is very efficient; its effectiveness is described in Section IV.

2) *Scenario 2- Increase in the TSMs of Backup Relays*: In some of the cases for which scenario 1 cannot solve the problem, scenario 2 is used. In this scenario, miscoordination pairs are detected, and to clear these undesirable cases, backup TSMs are increased in turn. Next, according to main relay TSMs and CTI, new greater values for backup relay TSMs are calculated. In the case that two or more violated constraints have the same backup relay, TSM of the backup relay is tuned so that all violations are cleared (i.e., the greatest calculated TSM is selected for the backup relay). Scenario 2 is implemented until all violations are cleared. Note that after any changes in TSMs, discrimination times are updated.

In summary, in scenario 1, TSM values of main relays in miscoordination pairs are reduced; in comparison, TSM values of backup relays in miscoordination pairs are increased in scenario 2. Thus, a holistic view shows that scenario 1 has more priority than scenario 2. Although raising the TSM values for backup relays has destructive effects on the primary operating times of relays, some insolvable miscoordinations can be quickly removed using this approach. Consequently, the GA-PSO and NLP parts can perform their duties much faster. Note that if the proposed algorithm works without scenario 1, because of scenario 2, many TSMs increase until all miscoordinations are removed. However, because of the uncontrolled increase in the TSM quantities, the whole algorithm becomes slow, and the feasibility of solutions might be ignored. Thus, after implementing scenario 1 and GA-PSO, scenario 2 is very efficient, and only one application of scenario 2 removes all miscoordinations quickly. The effectiveness of scenario 2 is shown in Section IV.

3) *Relay Type Determination*: This part is implemented when different relay curves are allowed. Typically, this part is performed using metaheuristic approaches in the literature. However, considering the discussed drawbacks of metaheuristic methods, these methods are very time consuming and inefficient for this end. If this task is performed manually in lower time, in addition to the decrease in total algorithm run time, the metaheuristic part becomes less constrained and can perform other duties with higher accuracy. The superiority of the proposed method becomes more prominent when different relay types are given for coordination because of this part. This fact is shown in Section IV. According to IEC standard 255-4 relay curves (see Table I), there are three alternatives for each relay curve. In this part, first, the global best population is selected. Next, based on its data, the cost function ( $O.F_1$ ) for each relay considering three curves is calculated. This action is performed for all relays, and the type of relay with the lowest corresponding cost function is updated. This task is iteratively continued until no relay type can be updated. As an illustrative example, consider the 8-bus IEEE network with 14 relays. Each relay type has three alternatives. The cost function is calculated for each relay for three cases; thus, for this network, 42 cost function calculations are required. After these calculations, the lower cost function identifies the relay whose type should be updated. After updating, the algorithm is continued until no relay type can be updated. Note that the location of this part in the proposed algorithm affects the performance of the algorithm significantly. To be exact, although there are several alternatives, when this part is implemented in the structure of RGP, the maximum efficiency can be achieved because of the discussed merits and the superiorities of RGP over other algorithms to find the local optima. This aspect is discussed in more detail in the next section. Note that in addition to the structure of RGP, if this part is executed after the metaheuristic part, then even better results can be achieved at the expense of a longer computer run time.

### C. Nonlinear Programming

There are two important considerations in the overcurrent coordination optimization problem. First, selecting an NLP



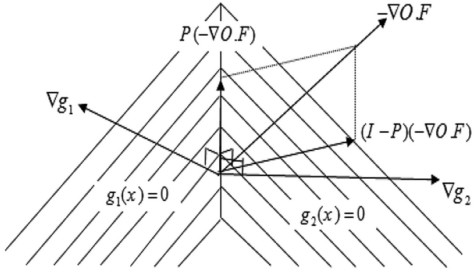


Fig. 2. Optimization instance assuming two constraints.

technique to optimize all PSMs and TSMs is not reasonable because, after optimization of TSMs and PSMs, GA-PSO clearly falls into local traps, and escaping from this situation and searching over the design space for global optima is generally not possible. Thus, the only reasonable solution is to optimize only TSMs and let the GA-PSO algorithm search for PSMs. Consequently, in addition to escaping from local optima, the advantages of metaheuristic methods can be exploited. Second, minimizing primary operation times, TSMs and discrimination times without creating any violation with an acceptable efficiency and accuracy are other important objectives of NLP. Consequently, the applied fitness function to NLP must be non-linear. The applied fitness function to NLP has been introduced as  $O.F_1$ , which satisfies NLP purposes without any attention to the miscoordination issue. According to the above-mentioned description, RGP and the complex method are some of the best choices for the NLP part of the proposed method as follows.

1) *Complex Method*: According to [39], to solve a nonlinear problem by using the complex method, considering  $n$  as the number of design variables,  $k$  initial points must be available, where  $k$  is equal or greater than  $n + 1$ . In other words, a population of at least  $n + 1$  without any miscoordination must be provided. Therefore, the population number in GA-PSO must be greater than this value. In each stage of the proposed algorithm, the GA-PSO operator sorts all populations based on their cost functions. If at least the first  $(n + 1)$ th chromosomes satisfy all constraints, then the complex method is applicable, and this is the entrance condition to the complex method. The complex method structure is based on the reflection process [39].

2) *Rosen's Gradient Projection*: RGP is an effective method to solve nonlinear problems with linear constraints and nonlinear objectives. If the provided initial conjecture by GA-PSO, i.e., the first population, is in a proper convex zone, then the steepest descent direction  $-\nabla(O.F_1)$  improves the current point substantially. As long as none of the constraints become active, moving along this direction leads to a decrease in  $O.F_1$ ; however, another issue is feasibility. Thus, considering constraint borders, reducing  $O.F_1$  is desirable; this goal can be performed by applying the projection vector. For further illustration, an optimization problem with two constraints is assumed. The instance is a three-dimensional optimization problem, see Fig. 2. For the current case, going along  $-\nabla(O.F_1)$  direction leads to violations in  $g_1(x)$  and  $g_2(x)$ .

To avoid these violations a new usable feasible direction  $(-P \cdot \nabla(O.F_1))$  with the following properties should be considered:

$$\nabla g_1 \cdot (-P \cdot \nabla(O.F_1)) = \nabla g_2 \cdot (-P \cdot \nabla(O.F_1)) = 0. \quad (9)$$

Therefore, we have

$$N_P \cdot (-P \cdot \nabla(O.F_1)) = 0 \quad (10)$$

where  $N_P$  consists of the gradient of all active constraints. In other words, the first and second columns of  $N_P$  are  $\nabla g_1$  and  $\nabla(g_2)$ , respectively.  $-\nabla(O.F_1)$  can be defined as

$$-\nabla(O.F_1) = -P \cdot \nabla(O.F_1) - [I - P] \cdot \nabla(O.F_1). \quad (11)$$

As indicated in Fig. 2, the second part of the right-hand side of (7) is in the hyperplane tangent of specific active constraints. Thus, it can be constructed by the gradient of particular active constraints by  $\lambda_1$  and  $\lambda_2$  coefficients as follows:

$$-[I - P] \cdot \nabla(O.F_1) = N_P^T \lambda, \text{ where } \lambda = \{\lambda_1, \lambda_2\}. \quad (12)$$

Multiplying (8) by  $N_P$  results in

$$-N_P [I - P] \cdot \nabla(O.F_1) = N_P N_P^T \lambda. \quad (13)$$

Thus,  $\lambda$  is given by

$$\lambda = -\left\{ (N_P N_P^T)^{-1} N_P \cdot \nabla(O.F_1) - (N_P N_P^T)^{-1} N_P P \cdot \nabla(O.F_1) \right\}. \quad (14)$$

Using (10) and (14) altogether, we have

$$\lambda = -\left\{ (N_P N_P^T)^{-1} N_P \cdot \nabla(O.F_1) \right\}. \quad (15)$$

According to (11), (12) and (15), we have

$$-\nabla(O.F_1) = -P \cdot \nabla(O.F_1) - N_P^T \left\{ (N_P N_P^T)^{-1} N_P \cdot \nabla(O.F_1) \right\}. \quad (16)$$

Thus

$$P = \left\{ I - N_P^T \left\{ (N_P N_P^T)^{-1} N_P \right\} \right\}. \quad (17)$$

In summary, we have

*Step 1*: All constraints should be inspected whether they are active (i.e., equal to zero). In the case of having an active constraint, the projection matrix (11) should be prepared. Otherwise, solve all  $g_i(x)$ s for  $x = X_i + \lambda_k S_i$  where  $j = 1, 2, \dots$  is the constraint number, and select  $\lambda_M = \min(\lambda_k)$  without violating any constraints.

*Step 2*: Check whether  $\frac{dO.F_1}{d\lambda}(\lambda_M)$  is positive. If so, then solve  $\frac{dO.F_1}{d\lambda} = 0$  for  $x = X_i + \lambda_k S_i$  as  $\lambda_0$ ; the new quantity of  $\lambda_i$  for the next iteration is  $\lambda_i = \lambda_0$ . Otherwise, the new quantity of  $\lambda_i$  for the next iteration is  $\lambda_i = \lambda_M$ .

*Step 3*: Set  $X_{i+1} = X_i + \lambda_k S_i$ , and check how many constraints are active. If there is more than one active constraint, then calculate the projection matrix as (11), and obtain the normalized  $S_i$  as follows:

$$S_i = \frac{-P \cdot \nabla(O.F_1(X_i))}{\|P \cdot \nabla(O.F_1(X_i))\|}. \quad (18)$$

If all constraints are feasible, set  $S_i$  as follows:

$$S_i = \frac{-\nabla(\text{O}\cdot\text{F}_1(X_i))}{\|\nabla(\text{O}\cdot\text{F}_1(X_i))\|}. \quad (19)$$

*Step 4:* If  $S_i$  is zero, according to (17), (18) for  $X_i$

$$P \cdot \nabla(\text{O}\cdot\text{F}_1) = \left\{ I - N_P^T \left\{ (N_P N_P^T)^{-1} N_P \right\} \right\} \cdot \nabla(\text{O}\cdot\text{F}_1) = 0. \quad (20)$$

Thus,  $\nabla(\text{O}\cdot\text{F})$  for  $X_i$  is as follows:

$$\nabla(\text{O}\cdot\text{F}_1) = N_P^T \left\{ - \left\{ (N_P N_P^T)^{-1} N_P \right\} \cdot \nabla(\text{O}\cdot\text{F}_1) \right\} = N_P^T \lambda. \quad (21)$$

If all arrays of  $\lambda$  are positive, then the Karush–Kuhn–Tucker [39] conditions are satisfied. Moreover, it can be deduced that all elements of  $\nabla(\text{O}\cdot\text{F}_1(X_i))$  are positive; thus,  $\text{O}\cdot\text{F}_1$  tends to increase such that the recently found point is the optimized solution. If there are some negative elements in  $\lambda$ , then the array with the most negative value should be removed, and a new  $N_P^T$  should be defined by considering the active constraints. Note that once the RGP method is implemented, PSMs are constant; in the case that various relay curves are allowed, relay types and also coordination constraints (5)–(8) are updated after calculating a new  $X_i$

$$g_j(X_i) = t_{mj} - t_{bj} + \text{CTI}; \quad j = 1, 2, \dots, PN \quad (22)$$

$$g_j(X_i) = \text{TSM}_{\min} - \text{TSM}_j; \quad j = PN+1, \dots, PN+RN \quad (23)$$

$$g_j(X_i) = \text{TSM}_j - \text{TSM}_{\max}; \quad j = PN+RN+1, \dots, PN+2RN. \quad (24)$$

When relay type determination is implemented in the structure of RGP, convex zones derived from the relay curves become more expanded, and constraint activation is less possible, which facilitates movement in the direction of steepest descent. As a result, by expanding convex zones, reaching the global optima becomes more possible, and by facilitating the movement in the direction of steepest descent, the global optima can be reached faster. In summary, based on the above outlines, the structure of the proposed algorithm is given as follows.

*Step 1:* Define all coefficients, e.g., maximum iteration and population numbers, PN, and RN. Moreover, determine the initial populations based on their boundaries.

*Step 2:* Apply parallel GA-PSO based on Section III-A.

*Step 3:* Identify relay types based on the discussed procedure in Section III-B3. If the maximum iteration is met, then quit the algorithm.

*Step 4:* Check whether there is any miscoordination for the first population with the lowest cost function. If not, then go to Step 6. If yes, then implement scenario 1 for this population.

*Step 5:* Check whether there is any miscoordination removal. If yes, then go to Step 2. If not, then perform scenario 2. Next, increase the iteration number by one.

*Step 6:* Check the number of the first populations without miscoordination to determine whether it is greater than the number of design variables (RN). If not, then go to the

next step. If so, then perform the complex method for valid k initial points for one cycle. Evaluate and then order the populations based on the OF. Increase the iteration number by one.

*Step 7:*  $i = 1$  and  $X_i = \text{pop}(1)$ .  $\text{position}(j)$ ,  $j = 1, 2, \dots, RN$ .

*Step 8:*  $i = i + 1$ . Find new  $X_i$  by executing RGP. If required, determine the optimum relay types based on Section III-B3.

*Step 9:* Increase the iteration number by one. If the RGP exit criterion is met, then go to Step 2. Otherwise, go to the previous step. Note that the populations are prepared for the complex method part in Step 6 and that the complex method is implemented in Step 7. Regarding the proposed algorithm, although the RGP exit criterion in Step 9 is discussed in the corresponding section, the projection matrix (P) may become singular in some cases when the number of activated constraints increases. In this case, the algorithm becomes sluggish in the RGP part; thus, the cost function for two consecutive  $X_i$  is calculated. If their differences are less than a small value (e.g.,  $10^{-15}$ ), then RGP is stopped. In order to have more clarification, all the aforementioned steps are shown in details in Fig. 3. It can be observed that the complex method is executed if at least we have  $RN + 1$  feasible population. Another term which can be observed from Fig. 3 is that scenario 2 is performed if at least one single miscoordination becomes available; however, scenario 1 cannot remove this miscoordination. In the next section, the proposed algorithm results are presented, and comparisons are provided to verify the superiority of the proposed algorithm.

#### IV. SIMULATIONS AND RESULTS

The proposed algorithm has been applied to both the 8-bus IEEE 150-kV transmission network depicted in Fig. 1, [41] and the 33-kV distribution part of the 30-bus IEEE network. The required fault data and topology of the 30-bus network have been provided in [33], [42], and Fig. 4. Two cases of overcurrent coordination were investigated. In case 1, all relays are SI. In case 2, the relay types given in Table I can be used. The results are shown in Tables II–VII. The distinction of the proposed method is highlighted in Table VIII. Also, the obtained total operating time for case 1 using only the GA-PSO is provided in this table. Several notable observations are discussed. First, the proposed method has been executed in a typical manner; better results may be achieved by additional executions. Table VIII indicates that although only normally inverse conventional DOCRs have been used for coordination, the results outperform that of the dual setting scheme in [35] and are in the range of the achieved results in [4] with minimal difference. This result indicates the reduction of excessive costs and equipment [35] and is an important result. Second, although scenario 2 removes all violations and is faster than scenario 1, scenario 1 eliminates violations by decreasing TSMs, while scenario 2 performs this task by increasing TSMs. Therefore, scenario 1 improves the process and constrains TSMs from achieving large values.

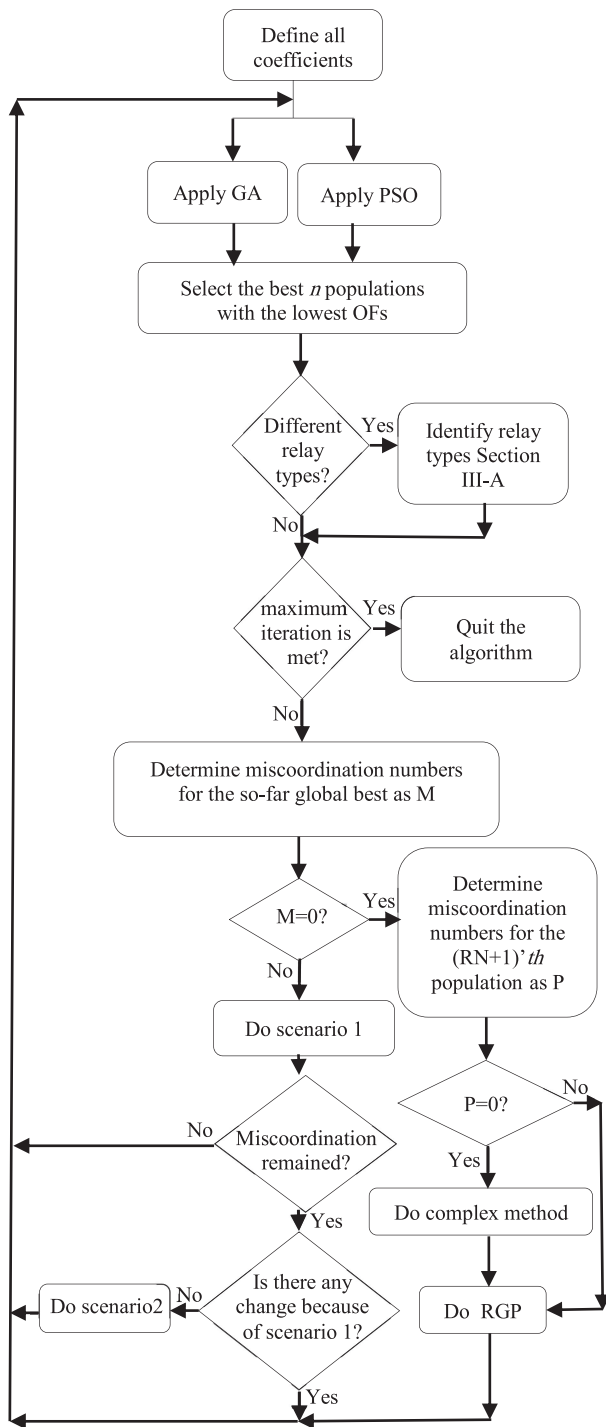


Fig. 3. Proposed algorithm flowchart.

Thus, the proposed method becomes robust and reliable and faster (e.g., 5 s for the 30-bus system) in the removal of violations (see Fig. 5). This robustness leads to another exclusive property that enables the proposed algorithm to remove violations in narrower bands of  $[TSM_{\min} \ TSM_{\max}]$  for which the GA-PSO part cannot remove violations in these bands. While this band becomes narrower, i.e., in the range of final optimized values for TSMs, another vital consequence for both cases can be achieved.

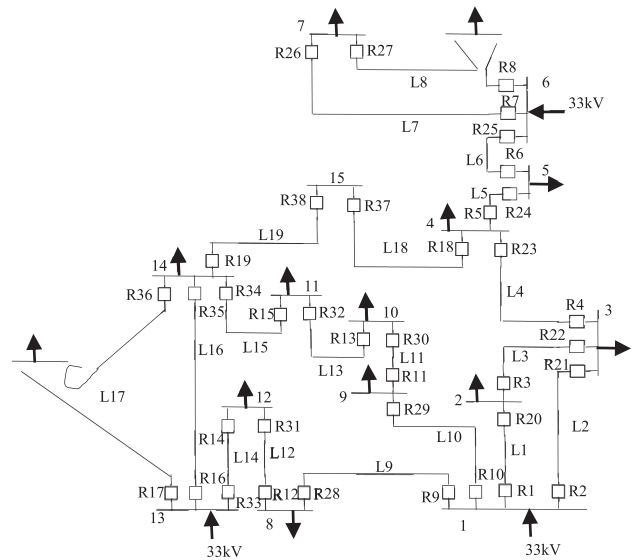


Fig. 4. 33-kV distribution portion of IEEE standard 30-bus network.

 TABLE II  
OBTAINED QUANTITIES FOR 8-BUS SYSTEM IN BOTH CASES

8-bus (case 1)				8-bus (case 2)				
RN	TSM	PSM	$t_{op-primary}$	RN	TSM	PSM	$t_{op-primary}$	
1	0.1135	1.3807	0.3907	1	0.0500	1.1583	0.1474	
2	0.1865	1.5821	0.6658	2	0.1410	0.9288	0.4656	
3	0.1553	1.5324	0.6113	3	0.0966	1.1371	0.3095	
4	0.1152	1.5674	0.5338	4	0.0800	0.9446	0.2695	
5	0.1152	1.3122	0.4715	5	0.0500	0.9433	0.1959	
6	0.1857	1.4267	0.5105	6	0.1332	1.1150	0.3962	
7	0.1383	1.5778	0.4723	7	0.1033	1.1412	0.3631	
8	0.1524	1.4584	0.4253	8	0.1350	1.0054	0.3845	
9	0.0635	1.6000	0.3210	9	0.0659	0.9381	0.2279	
10	0.1440	1.4140	0.4831	10	0.1281	0.8497	0.4146	
11	0.1628	1.3592	0.5908	11	0.1003	1.0314	0.2712	
12	0.2441	1.5257	0.7110	12	0.1572	1.0181	0.4564	
13	0.0703	1.5136	0.3040	13	0.0738	0.7097	0.1655	
14	0.1060	1.6000	0.4168	14	0.0932	0.9961	0.3413	
Sum of $t_{op-primary}$ (sec)				6.9077	Sum of $t_{op-primary}$ (sec) 4.4088			

 TABLE III  
OBTAINED RELAY TYPES FOR 8-BUS SYSTEM IN CASE 2

IEC SI	IEC VI	IEC EI
2-6-7-8-10-12-	1-3-4-9-13	5-11-14

 TABLE IV  
OBTAINED QUANTITIES FOR 30-BUS SYSTEM IN CASE 1

RN	TSM	PSM	$t_{op-primary}$	RN	TSM	PSM	$t_{op-primary}$
1	0.3375	1.3564	1.0749	20	0.0500	1.3316	0.2502
2	0.2783	1.4697	0.6931	21	0.0789	1.4265	0.2271
3	0.4383	1.3694	1.2289	22	0.1800	1.4206	0.5002
4	0.3026	1.3428	1.0553	23	0.1183	1.4059	0.5298
5	0.1971	1.4045	0.7194	24	0.1784	1.4095	0.9725
6	0.1590	1.3468	0.8731	25	0.2371	1.4597	0.9884
7	0.2761	1.3536	0.6014	26	0.0500	1.2000	0.2259
8	0.2908	1.4185	0.6194	27	0.0500	1.2000	0.1347
9	0.3895	1.3927	1.1466	28	0.1678	1.4355	1.1307
10	0.5281	1.5240	1.2601	29	0.2741	1.3383	0.9846
11	0.5086	1.3730	1.4253	30	0.3923	1.4117	1.1838
12	0.3854	1.4201	1.0614	31	0.3386	1.3438	1.1045
13	0.4409	1.3246	1.2448	32	0.3932	1.3899	1.2639
14	0.3331	1.3974	1.0712	33	0.4479	1.4877	1.0628
15	0.3744	1.4795	1.0909	34	0.5584	1.3600	1.2137
16	0.5046	1.4770	1.1568	35	0.3595	1.4748	0.9491
17	0.3123	1.4117	0.5757	36	0.3322	1.4558	0.5385
18	0.5854	1.3977	1.2150	37	0.3546	1.4089	0.7930
19	0.6479	1.3414	1.1253	38	0.6046	1.4841	1.2715
Sum of operation times = 34.5636 s							

TABLE V  
SAMPLES OF OBTAINED  $I_{pickup}$  FOR 30-BUS IN CASE 1

Relay Number	Pickup Current (A)	Relay Number	Pickup Current (A)
5	755.5788	15	278.1230
8	232.5991	25	743.8589
11	302.1110	33	367.5117

TABLE VI  
OBTAINED QUANTITIES FOR 30-BUS SYSTEM IN CASE 2

RN	TSM	PSM	$I_{top-primary}$	RN	TSM	PSM	$I_{top-primary}$
1	0.2778	1.2123	0.8400	20	0.0500	1.2603	0.2404
2	0.2154	1.4815	0.2036	21	0.0586	1.4644	0.1706
3	0.2993	1.4156	0.8512	22	0.3718	1.2961	0.4256
4	0.1871	1.4394	0.4450	23	0.0653	1.3674	0.2378
5	0.0845	1.4035	0.1603	24	0.0949	1.5527	0.5606
6	0.0500	1.4793	0.4314	25	0.1928	1.3142	0.5433
7	0.1454	1.3489	0.3163	26	0.0500	1.2000	0.2259
8	0.2680	1.4933	0.5805	27	0.0500	1.2000	0.0583
9	0.1877	1.4920	0.5698	28	0.1457	1.3510	0.9261
10	0.4003	1.5083	0.9516	29	0.2265	1.3468	0.5347
11	0.6292	1.4843	0.8861	30	0.4042	1.5189	0.6844
12	0.7431	1.2586	0.3296	31	0.3620	1.3751	0.6993
13	0.3943	1.4186	0.5602	32	0.4888	1.3459	0.5233
14	0.2434	1.3390	0.4219	33	0.5685	1.5219	0.4746
15	0.1498	1.5101	0.4404	34	0.6087	1.4197	0.3966
16	0.6297	1.3030	0.4056	35	0.3738	1.4364	0.1627
17	0.1712	1.4414	0.3174	36	0.2571	1.3610	0.0045
18	0.2946	1.4235	0.6151	37	0.4279	1.2983	0.2674
19	0.9871	1.4842	0.3128	38	0.7640	1.4262	0.4107
Sum of operation times = 17.1854 s							

TABLE VII  
OBTAINED RELAY TYPES FOR 30-BUS SYSTEM IN CASE 2

IEC SI	IEC VI	IEC EI
1-3-7-8-9-10-15-17-18-20-21-24-26-28	2-4-11-13-14-16-19-22-25-27-29-30-31-33-34-37-38	5-6-12-23-32-35-36

TABLE VIII  
COMPARISON TO OTHER COORDINATION METHODS

8-bus case 1		30-bus case 1	
Method	$\sum I_{top-primary}$	Method	$\sum I_{top-primary}$
Fuzzy-GA [12]	9.636 s	Dual setting-SQP [4]	34.172 s
Seeker [32]	8.427 s	Conventional-SQP [4]	64.172 s
QCQP [37]	21.89 s	[33] (two large violations)	22.25 s
Conventional GA [38]	11 s	Dual setting [35]	52.236 s
Hybrid GA-LP [38]	10.95 s	QCQP [37]	64.710 s
GA-PSO	10.67s	GA-PSO	69.75s
Proposed method	6.907 s	Proposed method	34.563 s

In case 1, the design space for TSMs is reduced, so, optimization quality is improved significantly. For case 2, in addition to this property, GA-PSO can be more relaxed and takes a specific opportunity to contribute to relay curve determination and PSM optimization. Although relay type determination is performed in its corresponding section, in that section, relay curves are determined by fixed values for TSMs and PSMs; in contrast, in the GA-PSO part, the variations of TSMs and PSMs are considered simultaneously for this end. Consequently, variations of relay curves cause greater changes in the OF; thus, GA-PSO concentrates more on relay types. This property makes the proposed method more prominent in case 2, as per Tables II and VI, and these superiorities are consequences of scenario 1 and scenario 2. The intervals [0.05, 0.2] and [0.05, 1] are used for the 8-bus and 30-bus, respectively. Third, the complex method is not

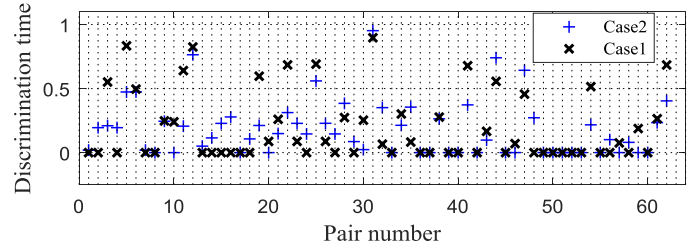


Fig. 5. Discrimination times for 30-bus system in different conditions.

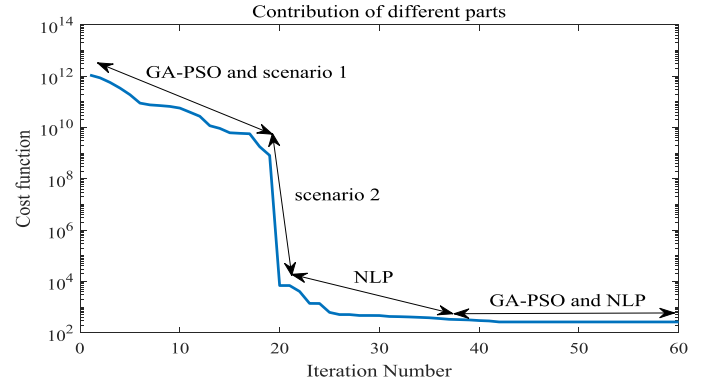


Fig. 6. Contribution of different parts in DOCRs coordination.

an appropriate alternative to combine with metaheuristic methods. In the complex method, a new solution can be determined by the central point and the worst point cost functions and reflection operator.

However, in metaheuristic techniques, all populations including the worst point move toward the best solution, and, depending on the weighting factors, all population chromosomes are quite near the best solution. Therefore, after several iterations, the best global solution and the worst solution become the same, and the reflection operator loses its application. Fourth, the results in Table VIII illustrate the unambiguous superiority of the proposed algorithm for large-scale and complex cases. A tenuous conclusion is that as the number of design parameters increases and the problem becomes more complex, the proposed algorithm becomes more practical and convenient because each duty has been assigned to its corresponding part. Fig. 6 shows that the GA-PSO and scenario 1 optimize all parameters; thus, if scenario 1 cannot remove violations and the GA-PSO algorithm falls into a trap, then scenario 2 takes the responsibility of removing all miscoordinations. After applying scenario 2, all the preconditions of the NLP algorithms are satisfied.

Note that in the RGP algorithm, all pickup currents are constant, and RGP optimizes only TSMs perfectly. After implementing RGP, as indicated in Fig. 6, the GA-PSO attempts to introduce new values for PSMs and TSMs. Fifth, the effectiveness of NLP can be observed in Fig. 6. After first-time RGP implementation, a near vicinity of the best possible solution is achieved, and improving this solution is very challenging to achieve in both GA-PSO and NLP parts. Moreover, the difference between NLP approaches, e.g., [4], and others, e.g.,



[35], can be observed from Table VIII for 30-bus coordination. Sixth, executing two metaheuristic methods in a parallel manner will enhance the exploration efficiency of the proposed method because entire opportunities for exploring better positions are considered. Once series combinations of two metaheuristic methods are executed; each population is delivered to only one metaheuristic method. Instead, all metaheuristic methods can examine their chances to explore a better position for each individual population in a parallel configuration. Seventh, the entire algorithm converges in 60 iterations and hence is not very time-consuming. Eighth, the GA-PSO algorithm can easily remove all miscoordinations when combined with scenarios 1 and 2. Moreover, the GA algorithm has an acceptable exploration level because of cross-over and mutation properties. In order to examine the accuracy and effectiveness of the proposed method; overcurrent coordination for the distribution portion of 30-bus IEEE standard test system considering a high DG penetration level should be performed. Also, the desirable performance of the proposed method should be scrutinized for both grid-connected and islanded operation modes. Based on Table VIII and also literature [6], [38], it can be clearly observed that deterministic approaches have superior exploitation, especially when larger power networks are considered for overcurrent coordination. Hence, to indicate the merits of the proposed method; the method should be compared with both conventional and dual setting (communication assisted) schemes for the aforementioned cases. Considering the above terms, the paper by Sharaf *et al.* [27] can be selected as an appropriate option to be compared with our proposed method. In [27], a new communication assisted dual setting has been proposed and applied to the modified 30-bus standard test system. In order to figure the same conditions in [27] for the modified 30-bus test system; 11 similar DG units are connected to the busbars 1, 2, 4, 6–8, 10–14. Each DG unit operates at unity power factor and is rated at 10 MVA and connected to the corresponding busbar by a 480 V/ 33 kV transformer. The modified version of the 30-bus network has 29 DOCRs and 51 relay pairs. It is worth mentioning that overcurrent coordination has been performed considering mid-way faults in [27] this is our case here in this part of the study as well. It can be found in Fig. 4 that the distribution section of the 30-bus network is fed through busbars 1, 6, and 13.

In case of islanding mode, these busbars are not fed from the 132 kV section of the 30-bus test system. In [27], MATLAB built-in optimization function *fmincon* is used as the optimizer engine while in this paper the entire parts of the proposed method have been programmed as a MATLAB code (i.e., m.file). Consequently, further modifications can be applied to the proposed method. For instance, the relay type determination or even the metaheuristic part can be executed in each loop of the RGP method. This modification leads to more improvement in the proposed method which is further illustrated by numerical examples. Thus, overcurrent coordination for both connected and islanded cases should be performed; however in each case, the obtained results by conventional (without communication links) coordination scheme (using the proposed optimization method and *fmincon* [27]) should be compared with communication

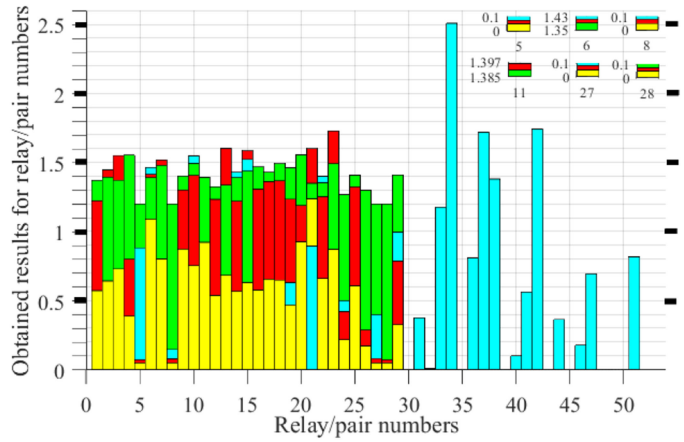


Fig. 7. Obtained results for case 3.

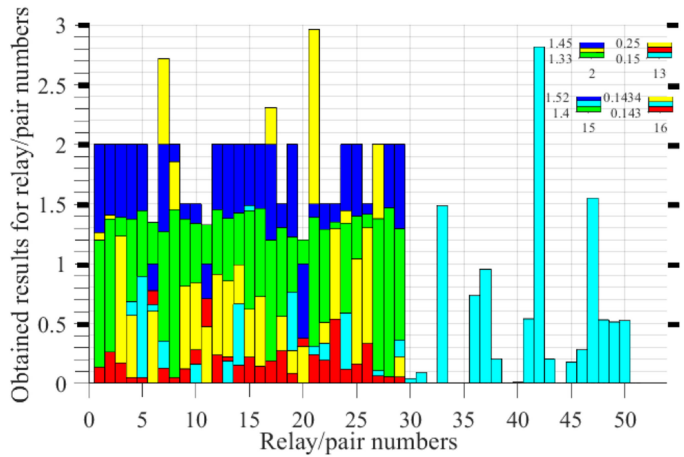


Fig. 8. Obtained results for case 4.

assisted dual setting scheme. In order to obtain more optimized results, the metaheuristic part is executed in each loop of the RGP method in the case that only SI relays are used. Also, both metaheuristic and the relay type determination process (mentioned in Section III-B 3) are executed in each loop of the RGP method where different relay types are allowed.

The proposed method is applied to the modified 30-bus IEEE test system for diverse configurations in following sections. Figs. 7–10 provide the obtained simulation results. These figures have some common properties. The obtained optimized values for TSMs, PSMs, relays operating times (for mid-way faults), and discrimination times are indicated in these figures by yellow, green, red, and light blue colors, respectively. Figs. 7 and 9 contain 138 data points whereas Figs. 8 and 10 contain 167 data points. In some cases that light blue bar charts do not exist for a specific relay pair, it means that discrimination time is zero for the corresponding pair. The first relay pair in all Figs. 7–10 is an example of this case. Relay numbering is the same with [27] and relay pairs are denoted by Table IX. Pair number, primary relay, and backup relay are denoted by PN, PR, and BR in Table IX.

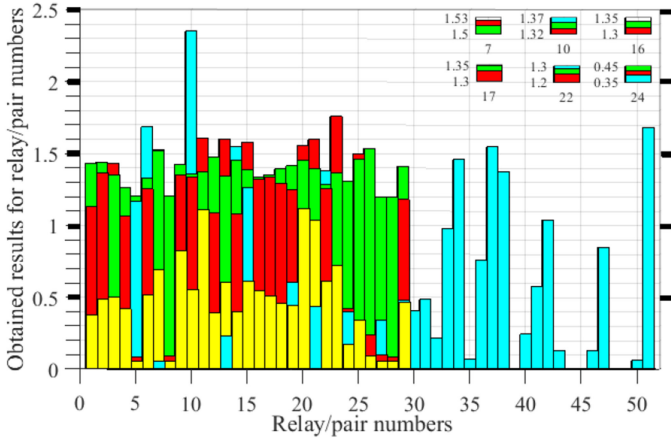


Fig. 9. Obtained results for case 5.

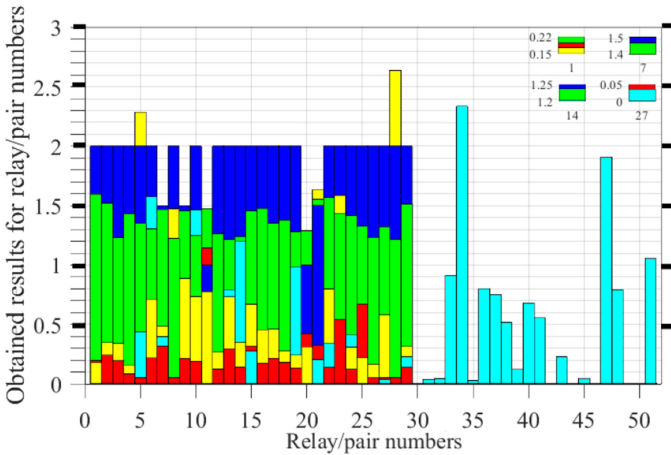


Fig. 10. Obtained results for case 6.

TABLE IX  
PAIR NUMBERS FOR MODIFIED 30-BUS SYSTEM

PN	PR	BR	PN	PR	BR	PN	PR	BR	PN	PR	BR
1	14	1	14	24	11	27	1	19	40	10	22
2	18	2	15	5	12	28	3	19	41	1	23
3	21	3	16	6	12	29	4	19	42	2	23
4	22	4	17	15	13	30	1	20	43	3	23
5	24	4	18	12	14	31	2	20	44	20	23
6	8	6	19	2	15	32	4	20	45	26	24
7	10	6	20	3	15	33	1	21	46	27	24
8	11	6	21	4	15	34	2	21	47	22	25
9	13	7	22	8	16	35	3	21	48	23	25
10	5	9	23	9	16	36	22	21	49	28	26
11	7	9	24	11	16	37	24	21	50	25	29
12	17	10	25	19	17	38	8	22	51	27	29
13	23	11	26	16	18	39	9	22			

### A. Grid-Connected Topology

In this topology, overcurrent coordination is performed for the modified 30-bus IEEE test system where the 33-kV portion was connected to the 132-kV section. Case 3 indicates coordination with only SI relays whereas case 4 indicates coordination with different relay types (see Table I). Simulation results for

cases 3 and 4 are given in Figs. 7 and 8, respectively. For convenience, SI, VI, and EI relays are denoted by 1, 1.5, and 2 values in case 4 (i.e., dark blue bar charts in Fig. 8). For more clarification, consider relay/pair number 10 in Fig. 8. Obtained values of TSMs, PSMs, and relay operating time (for mid-way fault) is 0.84 s, 1.34 s, and 0.28 s, respectively, for relay number 10. Also, discrimination time of pair number 10 (Table IX, (4) and Fig. 8) is 0.16 s. Some obtained values in case 4 are more than 3, however, y-axis in Fig. 8 is limited in [0, 3] boundary to preserve the resolution quality. The obtained TSMs of relays 5 and 28 are 3.82 s and 4 s, respectively. Also, the discrimination time of pair 34 is 5.91 s. It should be noted that the obtained type of relay 27 is EI which corresponds to the value of 2 for the dark blue bar chart in Fig. 8. On the other hand, the obtained value for TSM of the same relay is 2. Hence, the yellow bar chart height is the same with the dark blue bar chart height and consequently, the yellow bar chart lies on the dark blue bar chart in Fig. 8 for relay number 27. In the case of SI relays coordination, the total relays operating times for the conventional coordination scheme with MATLAB built-in *fmincon* optimizer and communication-assisted dual setting coordination scheme are 70.28 s and 30.94 s, respectively [27]. We observed a 55.9% reduction in case of the dual setting scheme. Now, applying the proposed optimizer engine to the conventional coordination scheme results in 31.87 s for total relays operating time (case 3) which corresponds to 55% reduction compared with *fmincon* optimizer engine. In the case that various relay curves are allowed (case 4), total relays operating times is 6.38 s which shows 79% reduction as compared with communication assisted dual setting approaches without any need to extra costs.

### B. Islanded Topology

In this topology, overcurrent coordination is performed for the modified 30-bus IEEE test system where the 33-kV section is disconnected from the 132-kV section. Case 5 indicates coordination with only SI relays whereas case 6 indicates coordination with different relay types (see Table I). Simulation results in cases 5 and 6 are given by Figs. 9 and 10, respectively. The only obtained variable which is greater than 3 in this topology is the discrimination time of pair 42 ( $=3.17$  s) in case 6. In the case of SI relays coordination, the total relays operating times for the conventional coordination scheme with MATLAB built-in *fmincon* optimizer and communication-assisted dual setting coordination scheme are 77.65 s and 32.24 s, respectively [27]. We observe 58.48% reduction in case of the dual setting scheme. Now, applying the proposed optimizer engine to the conventional coordination scheme results in 32.4 s for total relays operating time (case 5) which corresponds to 58.27% reduction as compared with *fmincon* optimizer engine. For the case that various DOCR curves are allowed (case 6), total relays operating times is 6.94 s that shows 78% reduction compared with communication-assisted dual setting approaches without any need to extra costs. The robust performance of the proposed method can be assured by these comparisons. It is worth noting that the final found solution by deterministic approaches highly depends on the initial point because the local

optima in the convex vicinity of the initial conjecture always are found by deterministic approaches. Hence, various initial points should be manually given to deterministic methods to avoid being trapped in local optima [27] which is not the case for the proposed method. In comparison, the obtained results using the proposed method are close to each other in different algorithm runs (average 35.7 s for 10 algorithm runs). Hence, various initial points cause no considerable differences in the final results.

A simple comparison confirms the robustness of the proposed method in cases that the metaheuristic and relay determination parts (mentioned in Section III-B 3) are executed in each loop of the RGP algorithm. The obtained total relays operating times for case 3 and case 5 are 31.87 s and 32.4 s which are lower than the obtained value in case 1 (34.56 s in Table IV). This difference can be more obvious when different relay types (see Table I) are allowed for overcurrent coordination. The obtained total relays operating times for case 4 and case 6 are 6.38 s and 6.94 s. Comparing these values with the obtained value in case 2 (17.19 s in Table IV) shows a great difference.

In this paper, a novel optimizer engine has been proposed to the conventional overcurrent coordination scheme. The results were satisfactory and also in the range dual setting communication assisted approaches results. Hence, excessive costs can be avoided in our proposed solution. Precise look to the performance, exploration and exploitation of other optimization methods (in particular, stochastic methods), these methods cannot overcome the proposed optimizer engine (for finding the global optima); no matter how much are their population, iteration and computational burdens and time.

## V. CONCLUSION

A novel algorithm was proposed to coordinate DOCRs for 8- and 30-bus IEEE systems. In this regard, the GA-PSO algorithm associated with RGP and some manual tunings has overcome the miscoordination issue in meshed power systems. As indicated, each part of the proposed algorithm has special duties, and this feature has led to enhance algorithm reliability, robustness, efficiency, and accuracy, particularly for large-scale coordination of DOCRs. The GA-PSO shares some overcurrent coordination tasks with NLP. Optimizing PSM design variables and inhibiting trapping in local optima without any violations are important goals of the GA-PSO algorithm. On the one hand, reducing the GA-PSO duties reduces some disadvantages of the metaheuristic part; on the other hand, exploration is preserved because of PSM optimization by GA-PSO. As indicated by the simulations and results, the exploitation of the proposed method is efficiently improved by implementing RGP for optimizing TSMs.

## REFERENCES

[1] M. E. Hamidi and R. Mohammadi Chabanloo, "Optimal allocation of distributed generation with optimal sizing of fault current limiter to reduce the impact on distribution networks using NSGA-II," *IEEE Syst. J.*, to be published.

[2] H. Yazdanpanahi *et al.*, "A new control strategy to mitigate the impact of inverter-based DGs on protection system," *IEEE Trans. Smart Grid*, vol. 3, no. 3, pp. 1427–1436, Sep. 2012.

[3] M. Y. Shih *et al.*, "An adaptive overcurrent coordination scheme to improve relay sensitivity and overcome drawbacks due to distributed generation in smart grids," *IEEE Trans. Ind. Appl.*, vol. 53, no. 6, pp. 5217–5228, Nov./Dec. 2017.

[4] H. H. Zeineldin *et al.*, "Optimal protection coordination for meshed distribution systems with DG using dual setting directional over-current relays," *IEEE Trans. Smart Grid*, vol. 6, no. 1, pp. 115–123, Jan. 2015.

[5] D. Solati Alkaran *et al.*, "Overcurrent relays coordination in interconnected networks using accurate analytical method and based on determination of fault critical point," *IEEE Trans. Power Del.*, vol. 30, no. 2, pp. 870–877, Apr. 2015.

[6] P. P. Bedekar and S. R. Bhide, "Optimum coordination of directional overcurrent relays using the hybrid GA-NLP approach," *IEEE Trans. Power Del.*, vol. 26, no. 1, pp. 109–119, Jan. 2011.

[7] S. Santoso and T. A. Short, "Identification of fuse and recloser operations in a radial distribution system," *IEEE Trans. Power Del.*, vol. 22, no. 4, pp. 2370–2377, Oct. 2007.

[8] A. F. Naiem *et al.*, "A classification technique for recloser-fuse coordination in distribution systems with distributed generation," *IEEE Trans. Power Del.*, vol. 27, no. 1, pp. 176–185, Jan. 2012.

[9] B. Hussain *et al.*, "An adaptive relaying scheme for fuse saving in distribution networks with distributed generation," *IEEE Trans. Power Del.*, vol. 28, no. 2, pp. 669–677, Apr. 2013.

[10] S. Chaitusaney and A. Yokoyama, "Prevention of reliability degradation from recloser–fuse miscoordination due to distributed generation," *IEEE Trans. Power Del.*, vol. 23, no. 4, pp. 2545–2554, Oct. 2008.

[11] V. C. Nikolaidis *et al.*, "A communication-assisted overcurrent protection scheme for radial distribution systems with distributed generation," *IEEE Trans. Smart Grid*, vol. 7, no. 1, pp. 114–123, Jan. 2016.

[12] D. S. Alkaran *et al.*, "Optimal overcurrent relay coordination in interconnected networks by using fuzzy-based GA method," *IEEE Trans. Smart Grid*, vol. 9, no. 4, pp. 3091–3101, Jul. 2018.

[13] S. M. Brahma and A. A. Girgis, "Development of adaptive protection scheme for distribution systems with high penetration of distributed generation," *IEEE Trans. Power Del.*, vol. 19, no. 1, pp. 56–63, Jan. 2004.

[14] M. Nabab Alam, "Adaptive protection coordination scheme using numerical directional overcurrent relays," *IEEE Trans. Ind. Informat.*, vol. 15, no. 1, pp. 64–73, Jan. 2019.

[15] F. Coffele *et al.*, "An adaptive overcurrent protection scheme for distribution networks," *IEEE Trans. Power Del.*, vol. 30, no. 2, pp. 561–568, Apr. 2015.

[16] P. Mahat *et al.*, "A simple adaptive overcurrent protection of distribution systems with distributed generation," *IEEE Trans. Smart Grid*, vol. 2, no. 3, pp. 428–437, Sep. 2011.

[17] Ł. Huchel and H. H. Zeineldin, "Planning the coordination of directional overcurrent relays for distribution systems considering DG," *IEEE Trans. Smart Grid*, vol. 7, no. 3, pp. 1642–1649, May 2016.

[18] E. Dehghanpour *et al.*, "Optimal coordination of directional overcurrent relays in microgrids by using cuckoo-linear optimization algorithm and fault current limiter," *IEEE Trans. Smart Grid*, vol. 9, no. 2, pp. 1365–1375, Mar. 2018.

[19] H. Samet *et al.*, "Efficient current-based directional relay algorithm," *IEEE Syst. J.*, to be published.

[20] M. M. Salem *et al.*, "Modified inverter control of distributed generation for enhanced relaying coordination in distribution networks," *IEEE Trans. Power Del.*, vol. 32, no. 1, pp. 78–87, Feb. 2017.

[21] R. Meyer *et al.*, "Fault ride through control of medium-voltage converters with LCL filter in distributed generation systems," *IEEE Trans. Ind. Appl.*, vol. 50, no. 5, pp. 3448–3456, Sep./Oct. 2014.

[22] H. Zhan *et al.*, "Relay protection coordination integrated optimal placement and sizing of distributed generation sources in distribution networks," *IEEE Trans. Smart Grid*, vol. 7, no. 1, pp. 55–65, Jan. 2016.

[23] S. Khanbabapour and M. S. Hamedani Golshan, "Synchronous DG planning for simultaneous improvement of technical, overcurrent and timely anti-islanding protection indices of the network to preserve protection coordination," *IEEE Trans. Power Del.*, vol. 32, no. 1, pp. 474–483, Feb. 2017.

[24] M. Ojaghi and V. Mohammadi, "Use of clustering to reduce the number of different setting groups for adaptive coordination of overcurrent relays," *IEEE Trans. Power Del.*, vol. 33, no. 3, pp. 1204–1212, Jun. 2018.

[25] L. Liu and L. Fu, "Minimum break point set determination for directional overcurrent relay coordination in large scale power networks via matrix computations," *IEEE Trans. Power Del.*, vol. 32, no. 4, pp. 1784–1789, Aug. 2017.



- [26] R. Armentano *et al.*, *The Internet of Things: Foundation for Smart Cities, EHealth, and Ubiquitous Computing*, 1st ed. Boca Raton, FL, USA: CRC Press, 2017.
- [27] H. M. Sharaf *et al.*, "Protection coordination for microgrids with grid-connected and islanded capabilities using communication assisted dual setting directional overcurrent relays," *IEEE Trans. Smart Grid.*, vol. 9, no. 1, pp. 143–151, Jun. 2018.
- [28] T. Soleymani Aghdam *et al.*, "Transient stability constrained protection coordination for distribution systems with DG," *IEEE Trans. Smart Grid.*, vol. 9, no. 6, pp. 5733–5741, Nov. 2018.
- [29] T. Soleymani Aghdam *et al.*, "Optimal coordination of double-inverse overcurrent relays for stable operation of DGs," *IEEE Trans. Ind. Informat.*, vol. 15, no. 1, pp. 183–192, Jan. 2019.
- [30] A. Srivastava *et al.*, "Optimal coordination of overcurrent relays using gravitational search algorithm with DG penetration," *IEEE Trans. Ind. Appl.*, vol. 54, no. 2, pp. 1155–1165, Mar./Apr. 2018.
- [31] W. K. A. Najy *et al.*, "Optimal protection coordination for microgrids with grid-connected and islanded capability," *IEEE Trans. Ind. Electron.*, vol. 60, no. 4, pp. 1668–1677, Apr. 2013.
- [32] T. Amraee, "Coordination of directional overcurrent relays using seeker algorithm," *IEEE Trans. Power Del.*, vol. 27, no. 3, pp. 1415–1422, Jul. 2012.
- [33] R. Mohammadi *et al.*, "Overcurrent relays coordination considering the priority of constraints," *IEEE Trans. Power Del.*, vol. 26, no. 3, pp. 1927–1938, Jul. 2011.
- [34] M. M. Mansour *et al.*, "A modified particle swarm optimizer for the coordination of directional overcurrent relays," *IEEE Trans. Power Del.*, vol. 22, no. 3, pp. 1400–1410, Jul. 2007.
- [35] A. Yazdanejadi *et al.*, "Dual-setting directional overcurrent relays for protecting automated distribution networks," *IEEE Trans. Ind. Informat.*, vol. 15, no. 2, pp. 730–740, Feb. 2019.
- [36] E. Purwar *et al.*, "A novel constraints reduction based optimal relay coordination method considering variable operational status of distribution system with DGs," *IEEE Trans. Smart Grid.*, vol. 10, no. 1, pp. 889–898, Jan. 2019.
- [37] V. A. Papaspiliotopoulos *et al.*, "A novel quadratically constrained quadratic programming method for optimal coordination of directional overcurrent relays," *IEEE Trans. Power Del.*, vol. 32, no. 1, pp. 3–10, 2017.
- [38] A. Saberi Noghahi *et al.*, "Considering different network topologies in optimal overcurrent relay coordination using a hybrid GA," *IEEE Trans. Power Del.*, vol. 24, no. 4, pp. 1857–1863, Oct. 2009.
- [39] S. S. Rao, *Engineering Optimization: Theory and Practice*, 4th ed. Delhi, India: New Age Int., 2009.
- [40] J. Gers and E. Holmes, "Protection of Electricity Distribution Networks," 3rd Edition, ser. IET power and energy series. Institution of Engineering and Technology, 2011.
- [41] V. N. Rajput and K. Pandya, "On 8-bus test system for solving challenges in relay coordination," in *Proc. IEEE ICPS Conf.*, Mar. 4–6, 2016.
- [42] Available [Online]: <http://www.ee.washington.edu/research/pstca/>



**Ahmad Darabi** was born in Kermanshah, Iran, in 1988. He received the B.S. degree from Razi University of Kermanshah, Kermanshah, Iran, and the M.S. degree from Amirkabir University of Technology (AUT), Tehran, Iran, in 2012 and 2015, respectively.

He is currently an Academic Staff with the Technical University of Kermanshah. His research interests include power system protection, power electronics, metaheuristic, and deterministic optimization techniques.



**Mehdi Bagheri** (M'12) received the M.Sc. degree in power engineering from Sharif University of Technology, Tehran, Iran, in 2007, and the Ph.D. degree from the University of New South Wales, Sydney, NSW, Australia, in 2014.

He joined the Iran Transformer Research Institute, Tehran, Iran, as a Research Engineer, and was the Head of the Test and Diagnostic Department between 2008 and 2010. From 2015 to 2016, he served as a Postdoctoral Research Fellow with the Department of Electrical Engineering, National University of Singapore, Singapore, working closely with Rolls-Royce Pte. Ltd. on condition monitoring and predictive maintenance of marine transformers and filters. He is currently an Assistant Professor with the Department of Electrical and Computer Engineering, Nazarbayev University, Astana, Kazakhstan. He is an Associate Editor with IEEE ACCESS JOURNAL and member of IEEE Dielectrics and Electrical Insulation Society. His research interests include field and marine applications of high-voltage engineering, condition monitoring and diagnosis of power transformers and electrical rotating machines, transients in power systems, smart grids, dynamic wireless charging of EV and power quality.



**Gevork B. Gharehpetian** (M'00–SM'08) received the B.S. (First Class Hons.) degree in electrical engineering from Tabriz University, Tabriz, Iran, in 1987, the M.S. (First Class Hons.) degree in electrical engineering from the Amirkabir University of Technology (AUT), Tehran, Iran, in 1989, and the Ph.D. (First Class Hons.) degree in electrical engineering from Tehran University, Tehran, Iran, in 1996.

As a Ph.D. student, he has received scholarship from DAAD (German Academic Exchange Service) from 1993 to 1996 and he was with High Voltage Institute of RWTH Aachen, Aachen, Germany. He has been holding the Assistant Professor position at AUT from 1997 to 2003, the position of Associate Professor from 2004 to 2007, and has been a Professor since 2007. The power engineering group of AUT has been selected as a Center of Excellence on Power Systems in Iran since 2001. He is a member of this center. He is the author of more than 1000 journal and conference papers. His teaching and research interest include smart grid, microgrids, FACTS and HVdc systems, and monitoring of power transformers and its transients.

Dr. Gharehpetian was selected by the Ministry of Science Research and Technology (SMRT) as the Distinguished Professor of Iran, by the Iranian Association of Electrical and Electronics Engineers (IAEEE) as the Distinguished Researcher of Iran, by Iran Energy Association (IEA) as the Best Researcher of Iran in the field of energy, by the SMRT as the Distinguished Researcher of Iran, and by The Academy of Science of the Islamic Republic of Iran as the Distinguished Professor of electrical engineering and was awarded the National Prize, in 2008, 2010, 2018, 2018, and 2019, respectively. Based on the Web of Science Database (2005–2015), he is among world's top 1% elite scientists according to ESI (Essential Science Indicators) ranking system. He is a Distinguished Member of CIGRE and IAEEE. Since 2004, he has been the Editor-in-Chief for the *Journal of IAEEE*.